3

Highly Ordered Nanohole Arrays in Anodic Porous Alumina

Hideki Masuda

Department of Applied Chemistry, Tokyo Metropolitan University, 1-1 Minamiosawa, Hachioji, Tokyo 192-03, Japan
Masuda-hideki@c.metro-u.ac.jp

3.1. INTRODUCTION

Anodic porous alumina, which is formed by the anodization of Al in appropriate acidic or basic electrolytic solutions [1–3], has recently attracted much interest as a starting material for the fabrication of several kinds of nanodevices due to its fine porous structure with high aspect ratio. The recent improvement in the degree of ordering of the anodic porous alumina [4–7] has increased the attractiveness of this material from the viewpoint of nanofabrication.

The geometrical structure of anodic porous alumina is schematically represented as a honeycomb structure consisting of a close-packed array of columnar alumina units called cells, each containing a central straight hole (Figure 3.1). The dimensions of the anodic porous alumina cells depend on the anodizing conditions [1,2]. The cell size, which is equivalent to the hole interval, is determined by the applied voltage used for the anodization; the cell size has a good linear relationship with the applied voltage [3]. The value of the constant of the cell size divided by the applied voltage is approximately 2.5 nm/V. The hole size is dependent on the electrolyte composition, temperature, period of anodization as well as applied voltage. The hole size is also controlled by the pore-widening treatment by dipping the porous alumina in an appropriate acid solution after the anodization. The cell size usually ranges from 10 to 500 nm and the hole size from 5 to 400 nm depending on the anodizing and post-anodizing conditions. The depth of the holes (thickness of the oxide films) has a good linear relationship with the period of the anodization.

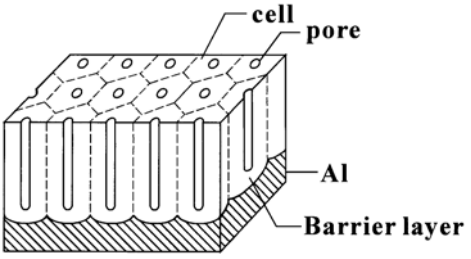

FIGURE 3.1. Schematic structure of anodic porous alumina.

3.2. NATURALLY OCCURRING LONG-RANGE ORDERING OF THE HOLE CONFIGURATION OF ANODIC ALUMINA

The ordering of the hole configuration of anodic porous alumina is essential for optimizing the performance of the obtained devices. The author and his coworkers have been studying the conditions for the naturally occurring long-range ordering of the hole configuration of anodic porous alumina in various kinds of acid electrolytes [4–7]. The long-range ordering of the hole configuration occurs under the appropriate anodizing conditions. The conditions of the long-range ordering are characterized by a long-period anodization under the appropriate constant anodizing voltages which are specific to the acid solution used for the anodization. The long-range ordering takes place at 25–27 V in sulfuric acid [5], 40 V in oxalic acid [4,6] and 195 V in phosphoric acid [7].

Figure 3.2 summarizes the SEM micrographs of the hole configuration with naturally occurring long-range ordering formed in these three acid electrolytes. These SEM micrographs were taken from the bottom side of the oxide layer called the barrier layer after the removal of the Al substrate with a saturated $HgCl_2$ solution. The barrier layer was removed with phosphoric acid solution, and then the pore-widening treatment was carried out using the same phosphoric acid solution. These treatments make it easy to observe the hole arrangement of the anodic porous alumina. In all of the SEM micrographs obtained in the three kinds of acids, the highly ordered hole configuration can be confirmed.

Figure 3.3 shows the dependence of the ordering of the hole configuration on anodizing period in sulfuric acid solution [5]. At the initial stage of the anodization, the holes develop randomly over the aluminium surface. During the growth of the oxide layer, the long-range ordering proceeds through the rearrangement of the hole configuration which changes gradually from a random configuration at the initial stage of anodization to a highly ordered configuration after the long-period anodization. In the hole configuration, characteristic patterns are observed in the array of holes as indicated by arrows (Figure 3.3a). These patterns correspond to the defect sites of the holes. As the ordering of the hole configuration proceeded, the number of these patterns decreased and an almost ideally ordered hole configuration was finally obtained over the sample [8–13].

From the large-area view (Figure 3.4), the ideally ordered area shows a domain structure at the boundary of which defects and imperfections are accumulated. During

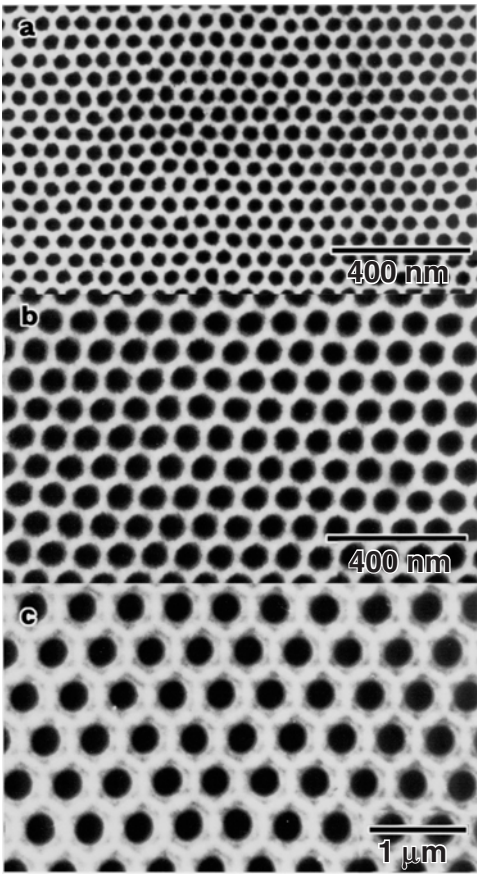

FIGURE 3.2. SEM micrographs of naturally occurring long-range ordered anodic porous alumina formed in three types of acid electrolytes: (a) sulfuric acid, (b) oxalic acid and (c) phosphoric acid.

the ordering of the hole configuration, such domains grow gradually, taking over the surrounding disordered holes, and attain an almost saturated size.

The manner of the self-ordering of hole configuration during anodization was almost the same in oxalic [4,6] and phosphoric acid [7] solutions except for the appropriate anodizing voltages. The saturated size of the ideally arranged domain is dependent on the size of the cells which compose the domain, i.e., it is largest in the phosphoric acid solution in which anodization is conducted under the highest applied voltage.

Concerning the naturally occurring self-ordering of the hole configuration of anodic porous alumina, similar results have been reported by other groups [8–12].

The detailed mechanism for explaining the dependence of the ordering on the applied voltage is not clear at the present stage. However, it appears that strain-free growth is feasible under the appropriate anodizing voltage.

FIGURE 3.3. Dependence of the ordering of the hole arrangement of anodic porous alumina on the anodizing period in 0.5 M sulfuric acid solution at 25 V: (a) 9 minutes, (b) 36 minutes and (c) 710 minutes.

3.3. TWO-STEP ANODIZATION FOR ORDERED ARRAYS WITH STRAIGHT HOLES IN NATURALLY ORDERING PROCESSES

The degree of the ordering of the hole configuration at the surface of the anodic porous alumina is low because the holes develop randomly at the initial stage of the anodization. To improve the ordering of the surface side of the anodic porous alumina, two-step anodization is effectively adopted [6]. The process involves two separate anodization processes: the first anodization process consists of a long-period anodization to form the highly ordered hole configuration at the oxide/Al interface and the second

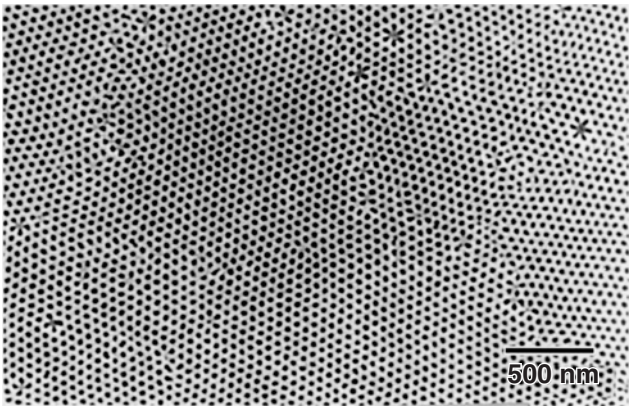

FIGURE 3.4. Low magnification SEM view of the long-range ordered anodic porous alumina formed in sulfuric acid at 25 V.

anodization is performed after the removal of the oxide formed in the first anodization step (Figure 3.5). After the removal of the oxide, an array of highly ordered dimples was formed on the Al, and these dimples can act as initiation sites for the hole development in the second anodization. This process generates an ordered hole array throughout the entire oxide layer. This process can also be applied for the preparation of a porous alumina mask used for several types of nanofabrication techniques in which the ordered straight through-holes are essential.

3.4. IDEALLY ORDERED HOLE ARRAY USING PRETEXTURING OF A1

In the case of the naturally occurring long-range ordering of the anodic porous alumina, the defect-free area forms the domain structure, and the size of the domain is limited to several micrometres. To form the ideally ordered single-domain structure over the sample, a new process using pretexturing of Al has been developed [14–16]. In this process, an array of shallow concaves is formed on Al by imprinting using a mould, and these concaves serve as initiation sites for the hole development at the initial stage of the anodization (Figure 3.6).

The master mould with a hexagonal array of the convexes was prepared by conventional electron beam (EB) lithography. The substrate used for the mould is a SiC single crystal wafer which has the mechanical strength and smoothness required for the mould.

The SiC mould is placed on the Al sheet, and pressing is conducted using an oil press at room temperature. After the imprinting, the pattern is fully transferred to the Al surface due to the sufficient plasticity of Al for mechanical moulding.

Figure 3.7 shows the SEM micrograph of the anodic porous alumina after the anodization of Al with a textured pattern [14]. In Figure 3.7, half of the sample (left-hand side) was pretextured using the mould. In the textured area, an ideally ordered hole configuration was formed, while the hole development was random in the untextured area.

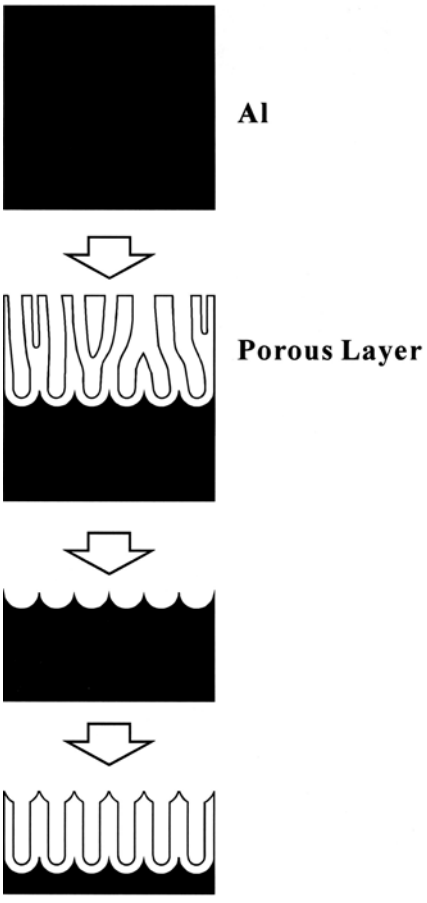

FIGURE 3.5. Schematic diagram of two-step anodization for the preparation of anodic porous alumina with straight holes.

Figure 3.8a shows the cross-sectional view of the sample of the single-domain structure. A highly ordered hole configuration and straight hole shape are confirmed throughout the film. The aspect ratio of the hole (hole length divided by the hole diameter) is approximately 150 in the sample of Figure 3.8. From the bottom side view shown in Figure 3.8b, it is confirmed that the ideally ordered hole configuration was maintained even at the bottom side of this high aspect ratio sample.

The lower limit of the dimensions of the fabrication of the hole array in the obtained structure is basically determined by the resolution of the patterning for the mould used for the imprinting. Figure 3.9 shows the SEM micrograph of the single-domain hole array with 63 nm interval which has the smallest period of holes at the present stage [15]. In the case of the sample in Figure 3.9, the hole size was 40 nm due to the post-etching treatment in phosphoric acid solution. The pore size was 15 nm in the case of the as-anodized sample without any pore-widening treatment.

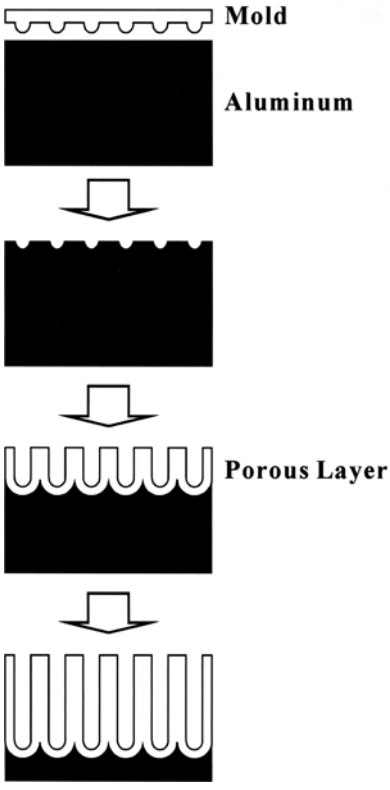

FIGURE 3.6. Schematic drawing of the preparation of anodic porous alumina with ideally ordered hole configuration using pretexturing process.

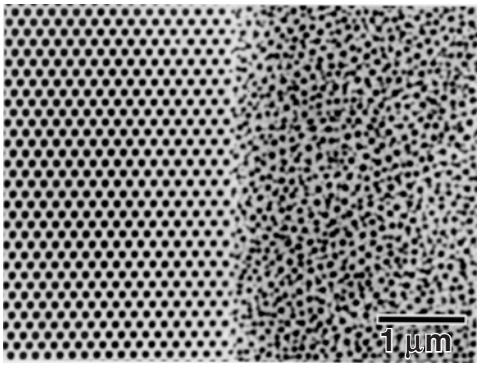

FIGURE 3.7. SEM micrograph of the surface of the anodic porous alumina using pretexturing process (left: prepatterned, right: no prepatterning).

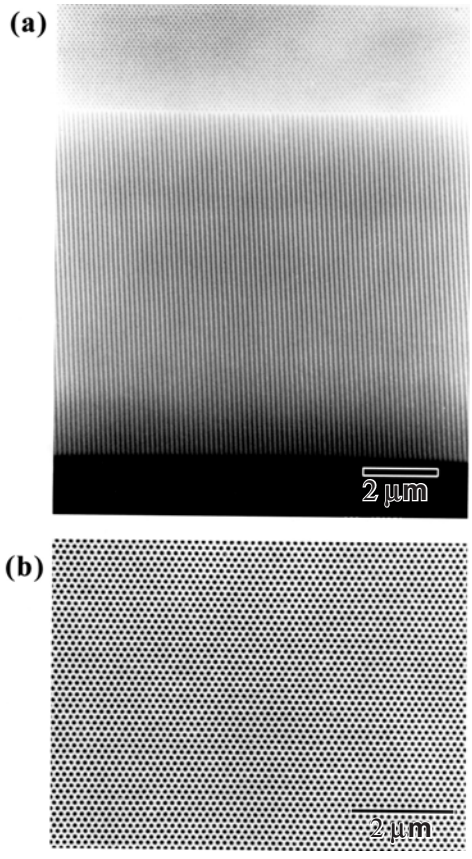

FIGURE 3.8. SEM micrographs of an ideally ordered anodic porous alumina: cross-sectional view (a) and bottom side view (b).

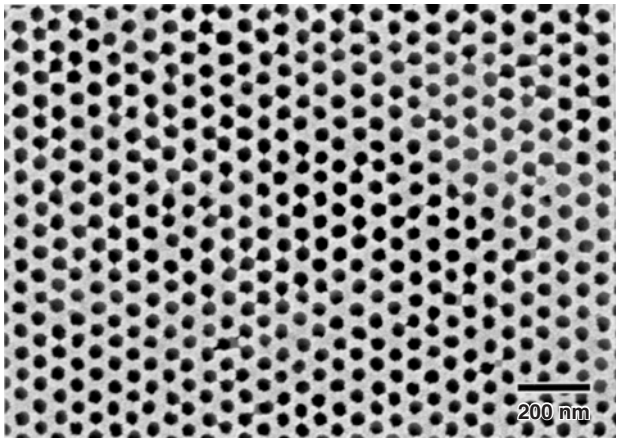

FIGURE 3.9. SEM micrograph of the ideally ordered anodic porous alumina with 63 nm hole interval.

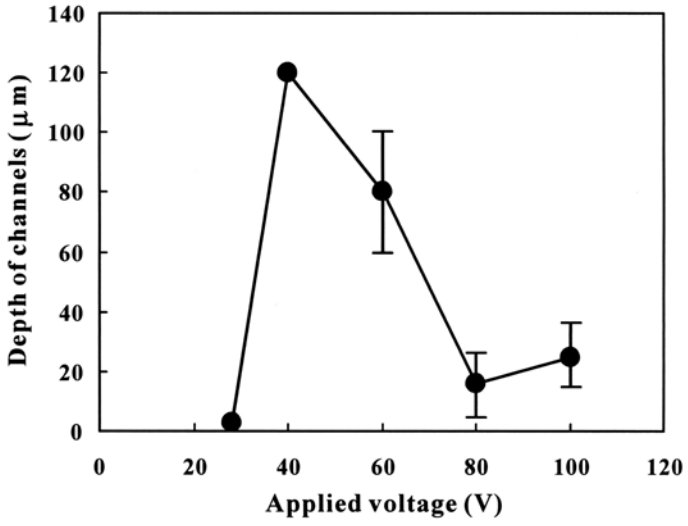

FIGURE 3.10. Dependence of the depth of holes with ideal ordering on the applied voltage for anodic porous alumina in oxalic acid.

Even in the case of anodization using the pretexuring of Al, appropriate anodizing conditions are essential for the fabrication of a hole array structure with a high aspect ratio [15,16]. Figure 3.10 shows the dependence of the depth of the ordered holes on the applied voltage for the anodization in oxalic acid solution [16]. Figure 3.10 shows that the most appropriate voltage for maintaining the ideal ordering is 40 V, and the ideal hole configuration with high aspect ratio cannot be maintained under other applied voltages. This voltage is in good accordance with the most appropriate voltage for the naturally occurring ordering in the oxalic acid. This result implies that the condition for the naturally occurring ordering is also important for maintaining the ideally ordered hole configuration induced by the pretexturing of Al.

Control of the hole development in anodic porous alumina by the use of a pretexturing process has also been reported by other groups. Liu *et al.* used the fast ion beam (FIB) technique for preparing the array of concaves on Al, which act as initiation sites for the hole development, and obtained the ideally ordered hole configuration of anodic porous alumina [17].

3.5. SELF-REPAIR OF THE HOLE CONFIGURATION IN ANODIC POROUS ALUMINA

One of the unique properties of anodic porous alumina is the self-repair of the hole configuration based on the self-compensation properties [18]. In the case of the anodization of pretextured Al using an imprinting process, even at the deficiency sites of the concaves, holes can be compensated automatically and an almost perfect arrangement of the hole configuration is generated. This is because that even at the deficiency sites, holes developed and then the closest packing of the cylindrical cells was recovered automatically.

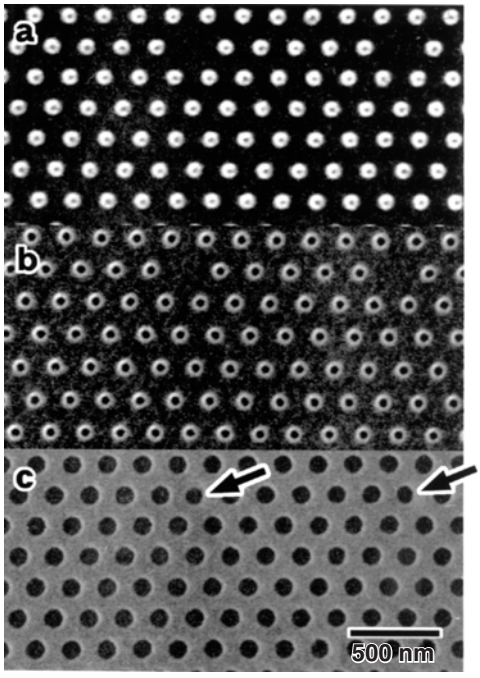

FIGURE 3.11. Self-repair of the hole configuration in anodic porous alumina: (a) SiC mould used for pretexturing, (b) pretextured Al and (c) anodic porous alumina with compensated holes at deficiency sites.

Figure 3.11 shows the results of the self-repair of the ordered pattern in anodic porous alumina [18]. In this experiment, the model pattern, in which some defects were introduced intensively, was used (Figure 3.11a). Figure 3.11b shows the SEM micrograph of the Al after the imprinting using a SiC mould with some defects in the pattern. After the anodization, the development of the holes could be observed even in the deficiency sites as shown by the arrows (Figure 3.11c). Using such a repaired structure as a template, moulds with a perfect arrangement of convexes for imprinting could be fabricated with metal.

This process is useful for the recovery of defects generated in the conventional lithographic processes and contributes to the fabrication of the defect-free fine pattern over a large area.

3.6. MODIFICATION OF THE SHAPE OF HOLE OPENING IN THE ANODIC POROUS ALUMINA

The shape of the cells of the anodic porous alumina can be determined by the mathematical expression known as the Voronoi tessellation. In the Voronoi tessellation, the pattern can be generated by a polygon, the boundary of which is a perpendicular bisector of two adjacent nuclei. In the naturally formed anodic porous alumina, the shape of the Voronoi cell is a hexagon with a triangular lattice. If the initiation nuclei sites can be laid out in other lattices, other cell shapes can be expected to form based

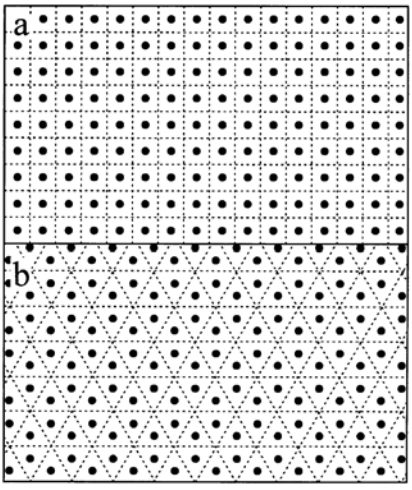

FIGURE 3.12. Formation of square and triangular cells based on Voronoi tessellation by controlling the layout of initiation site for the hole development.

on the Voronoi tessellation [19]. The shape of the cells is square in the square lattice and triangular in the graphite lattice, respectively (Figure 3.12). For the layout of the initiation site, the pretexturing process using a mould is successively used.

Figure 3.13 shows the SEM micrograph of the obtained anodic porous alumina with square and triangular openings [19]. The shape of the holes in the as-anodized

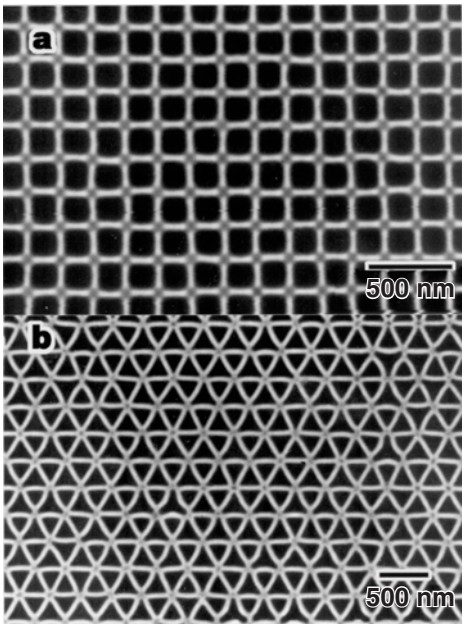

FIGURE 3.13. SEM micrographs of anodic porous alumina with square (a) and triangular holes (b).

anodic porous alumina was circular. However, the shape of the opening was changed from circular to square or triangular corresponding to the cell shape after the post-etching treatment in a phosphoric acid solution.

The most important concept of this process is that the shape of the obtained constituent units (cells, and cross section of holes) is determined by the arrangement of the nuclei in the two-dimensional space. This concept contributes to a higher resolution than that by the conventional pattering process where the pattern is formed through the painting of the figures by a stylus of limited size.

3.7. NANOFABRICATION BASED ON HIGHLY ORDERED ANODIC ALUMINA

3.7.1. 2D Photonic Crystals Using Anodic Porous Alumina

One of the promising application fields of the highly ordered hole array structure of the anodic porous alumina is two-dimensional (2D) photonic crystals (also see Chapter 7 by Wehrspohn and Schilling). The photonic crystals have a specially periodic refractive index with a lattice constant on the order of the wavelength of light, and show unique light propagation properties which can be used for the design of novel optoelectronic devices [20]. Works on the fabrication of 2D photonic crystals in the near infrared or visible wavelength are limited because of the difficulty in the fabrication of the ordered periodic structure with high aspect features. The geometrical structure of anodic porous alumina with an ordered array of air cylinders of a triangular lattice is one of typical 2D photonic crystals composed of air cylinders with a triangular lattice in an alumina matrix [21–23]. Photonic crystals based on anodic porous alumina are convenient to prepare and it is easy to control their dimensions.

The samples were cut in the specific directions in the air cylinder array, Γ–X, Γ–J (Figure 3.14), and optical measurement was carried out using a polarized light of E (E field paralleled to the air cylinders) and H (H field paralleled to air cylinders). Figure 3.15 shows the typical optical properties of the 2D photonic crystal prepared from the anodic porous alumina [21]. Distinct dips in the transmission spectra were observed for H polarization incident light in both Γ–X, and Γ–J directions, and an overlap wavelength region was observed. This dip in the transmission spectra was in good agreement with the calculation results for the hole array structure of anodic porous alumina. These results confirm that the anodic porous alumina with an ideally ordered hole configuration shows a photonic band gap in the visible wavelength region.

In addition to the ideally ordered anodic porous alumna obtained using the pretexturing process, naturally occurring ordered porous alumina also shows the photonic band gap corresponding to the hole period [23]. In this case, anodic porous alumina with the domain structure is interpreted as a polycrystalline type of photonic crystal.

3.7.2. Nanocomposite Using Highly Ordered Anodic Porous Alumina

There have been a large number of reports on the preparation of nanocomposite or nanocylinder structures using anodic porous alumina as a template [24–33]. The improvement of the hole configuration by naturally occurring long-range ordering of

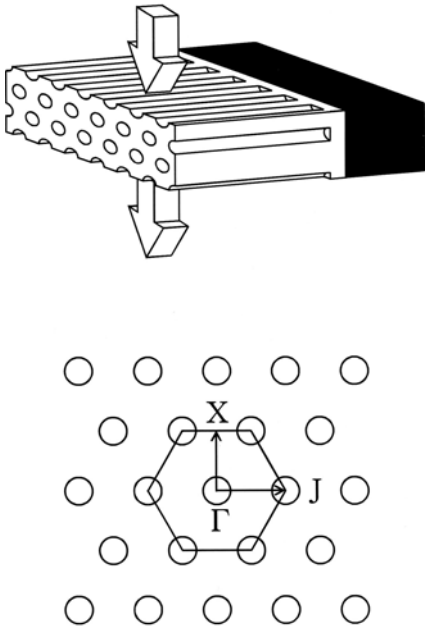

FIGURE 3.14. Top: Schematic diagram of the measurement configuration of 2D photonic band gap in anodic porous alumina. Bottom: Brioullinzone-free hexagonal porous alumina.

anodic porous alumina contributes to the advancement of the performance of the obtained nanodevices [34–41].

One of the promising application fields of the highly ordered anodic porous alumina is for the preparation of the array of electron emitters in which uniform-sized carbon nanotubes are imbedded in the holes of anodic porous alumina [35–37]. An ordered hole

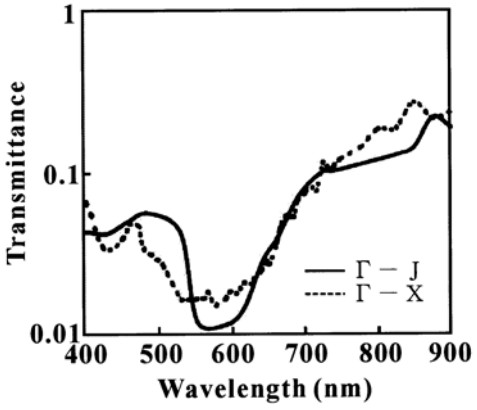

FIGURE 3.15. Transmission spectra of anodic porous alumina with 250 nm hole interval for *H*-polarized incident light.

array of anodic porous alumina was also used for CVD synthesis of nanocylindrical diamond [42].

Another application field of the long-range ordered anodic porous alumina is the fabrication of magnetic recording media [38–41] (see Chapter 8 by Nielsch *et al.*) Deposition of a ferromagnetic material such as Co or Ni into the micropores with high aspect ratio generates high-density perpendicular magnetic recording media. Although there have been large numbers of the reports on the magnetic recording media using anodic porous alumina [43,44], a highly ordered hole configuration contributes to the improvement of the S/N ratios of magnetic recording media using an anodic porous alumina matrix.

3.7.3. Two-Step Replication Process of the Hole Array Structure of Anodic Porous Alumina

Anodic porous alumina has several disadvantageous points in terms of its application in several areas: frangibility, low chemical stability, non-conductivity and so on. To overcome these disadvantageous points, and to expand the application fields of the anodic porous alumina, a new type of process, the so-called two-step replication process, has been developed [4,45–53]. This process consists of two main steps: the fabrication of a negative type of anodic porous alumina with a polymer (typically polymethylmethacrylate (PMMA)) and the subsequent reproduction of a positive type having an identical geometrical structure to starting anodic porous alumina (Figure 3.16). The important feature that distinguishes the present process from the usual one-step embedded process is that it permits the full replication of the hole array structure of anodic porous alumina and yields ordered hole array structures with desired materials.

For the preparation of the metal (Au, Ag, Pt, Ni, Pd, etc.) hole arrays, the electrochemical or electroless deposition of metals is adopted. Figure 3.17 shows the SEM micrograph of the typical hole array of Pt obtained by this process [4]. This process is also applied for the preparation of semiconductor hole array structures. Sol–gel deposition (TiO_2) [51] and electrochemical deposition (TiO_2, CdS) [52,53] are used for the injection of the semiconductors into the negative-type PMMA, and a semiconductor with ordered hole configuration is obtained.

This process has also been applied for the fabrication of nanohole arrays with other materials [54,55].

The obtained hole arrays are utilized as functional electrodes, sensors and photovoltaic cells. The hole array structure replicated with a high refractive index will also be useful as 2D phonic crystals in which a high contrast of refractive index is essential for obtaining the wide photonic band gap.

3.7.4. Fabrication of Nanodot and Nanohole Arrays Using Porous Alumina Masks

Anodic porous alumina with ordered straight through-holes can be applied to the mask for the fabrication of the nanodot or nanohole arrays [6,56–58]. After the anodization, the through-hole membrane is formed by removing the Al layer in a saturated $HgCl_2$ solution followed by the subsequent etching of the barrier layer in phosphoric acid

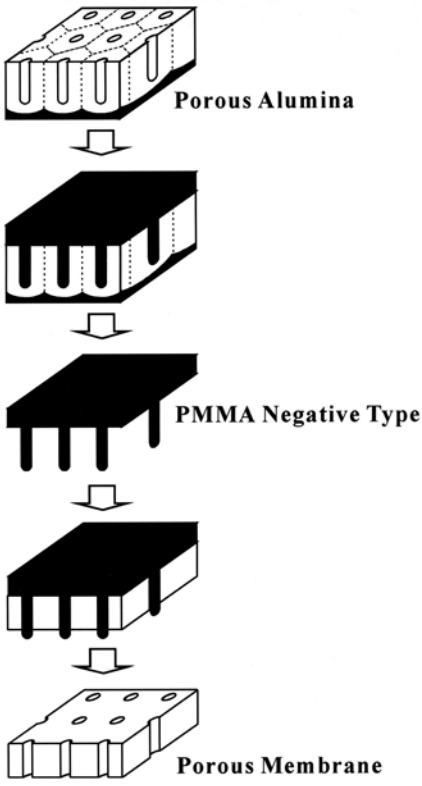

FIGURE 3.16. Two-step replication process using anodic porous alumina via PMMA negative.

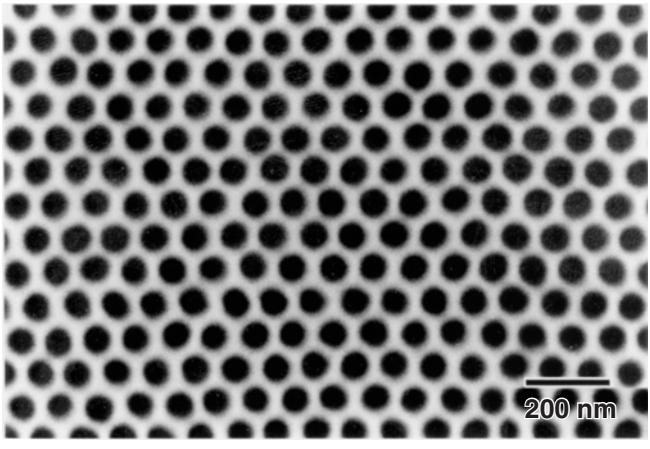

FIGURE 3.17. SEM micrograph of Pt hole array formed by two-step replication.

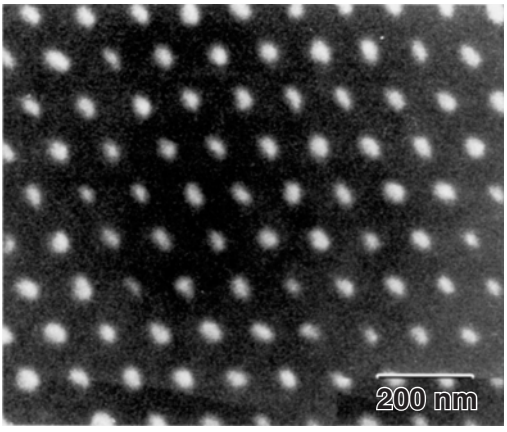

FIGURE 3.18. Nanodot array of Au on Si formed using anodic porous alumina mask with straight through-holes.

solution [6]. Two-step anodization is effective for the preparation of straight through-holes required for the mask applications in the case of naturally occurring anodic porous alumina [6].

The nanofabrication process using an anodic porous alumina mask is advantageous for the conventional lithographic process in the following: (1) a very fine pattern can be obtained over a large area, (2) the dimensions of the obtained structures can be controlled by changing the geometry of the anodic porous alumina mask and (3) the mask has holes with a high aspect ratio compared to the resist mask used in the conventional lithographic process.

Figure 3.18 shows the SEM micrograph of the metal (Au) nanodot array prepared on a Si substrate using an anodic porous alumina mask [6]. Au of 50 nm thickness was deposited through the anodic porous alumina mask using electron beam vacuum evaporation. The size and interval of the Au dots almost correspond to that of the alumina mask.

Making the characteristic feature of the alumina mask with a high aspect ratio, an array of multiple dots can also be fabricated based on the shadowing effect [56]. The sequential deposition of metals by changing the incidence angle yields an array of multiple metal dots on the substrate. The obtained array of multiple dots of nanometre dimension can be applied to the preparation of optical devices or model catalysts which requires an ordered array of multiple metal dots with nanometre dimensions.

The through-hole anodic porous alumina can also be used as a mask for the dry etching of several kinds of substrates [57–59]. The high resistance of the anodic porous alumina for the reactive etching plasma in addition to its high aspect ratio feature contributes to the fabrication of a hole array with high aspect ratio.

The use of the self-standing anodic porous alumina mask is simple and easy to perform on any type of substrates. However, the reproducibility and uniformity are insufficient because of the low adhesion of the mask to the substrates. To improve the adhesion of the mask to the substrates, the use of porous alumina prepared from the

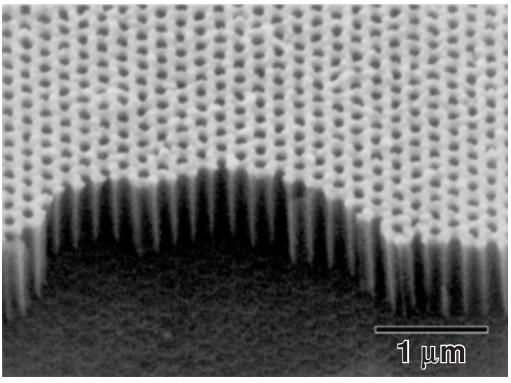

FIGURE 3.19. Anodic porous alumina mask on Si with an ideally ordered hole configuration obtained by anodization of pretextured Al on Si.

vacuum-evaporated Al was also used [9,35,58,60,61]. This process yields the mask preparation with high reproducibility and uniformity. An imprinting process using a mould is also applied to the Al on Si substrates, where the imprinting of Al is conducted using a SiC mould with hexagonally arranged convexes [58]. Figure 3.19 shows the SEM micrographs of the alumina mask prepared on a Si substrate using the imprinting process. The geometrical structure of the bottom part of the barrier layer on Si was different from that in bulk Al, that is, the shape of the barrier layer prepared from the Al/Si systems has voids beneath the pores [60]. This unique structure makes it easy to remove the barrier layer and generate the through-holes by the post-etching treatment in phosphoric acid solution.

3.8. CONCLUSION

Anodic porous alumina with highly ordered structures could be formed based on two types of ordering processes: naturally occurring ordering under the appropriate anodizing conditions and anodization using pretextured Al. The fabrication based on the naturally occurring long-range ordering is simple and useful for the ordered hole array configuration with large area. Anodic porous alumina with an ideally ordered hole array obtained by the pretexturing process is useful for applications in which a strictly ordered single-domain hole configuration is required, such as optical devices or patterned recording media. Both types of ordered anodic porous alumina are promising as starting structures for the fabrication of a wide variety of functional devices with nanometre dimensions.

REFERENCES

[1] F. Keller, M. Hunter and D.L. Robinson, J. Electrochem. Soc. **100**, 411 (1953).
[2] J.P.O'Sullivan and G.C. Wood, Proc. R. Soc. Lond., Ser. A **317**, 511 (1970).

[3] K. Ebihara, H. Takahashi and M. Nagayama, J. Surf. Fin. Soc. Jpn. **34**, 548 (1983).
[4] H. Masuda and K. Fukuda, Science **268**, 1466 (1995).
[5] H. Masuda, F. Hasegawa and S. Ono, J. Electrochem. Soc. **144**, L127 (1997).
[6] H. Masuda and M. Satoh, Jpn. J. Appl. Phys. **35**, L126 (1996).
[7] H. Masuda, K. Yada and A. Osaka, Jpn. J. Appl. Phys. **37**, L1340 (1998).
[8] S. Shingubara, O. Okino, Y. Sayama, H. Sakaue and T. Takahagi, Jpn. J. Appl. Phys. **36**, 7791 (1997).
[9] S. Shingubara, O. Okino, Y. Sayama, H. Sakaue and T. Takahagi, Solid-State Electron. **43**, 1143 (1999).
[10] O. Jessensky, F. Muller and U. Gosele, Appl. Phys. Lett. **72**, 1173 (1998).
[11] A.P. Li, F. Muller, A. Birner, K. Nielsch and U. Gosele, J. Appl. Phys. **84**, 6023 (1998).
[12] F. Li, L. Zhang and R.M. Metzger, Chem. Mater. **10**, 2470 (1998).
[13] L. Zhang, H.S. Cho, F. Li, R.M. Metzger and W.D. Doyle, J. Mater. Sci. Lett. **17**, 291 (1998).
[14] H. Masuda, H. Yamada, M. Satoh, H. Asoh, M. Nakao and T. Tamamura, Appl. Phys. Lett. **71**, 2770 (1997).
[15] H. Asoh, K. Nishio, M. Nakao, A. Yokoo, T. Tamamura and H. Masuda, J. Vac. Sci. Tech. B **19**, 569 (2001).
[16] H. Asoh, K. Nishio, M. Nakao, T. Tamamura and H. Masuda, J. Electochem. Soc. **148**, B152 (2001).
[17] C.Y. Liu, A. Datta and Y.L. Wang, Appl. Phys. Lett. **78**, 120 (2001).
[18] H. Masuda, M. Yotsuya, M. Asano, K. Nishio, M. Nakao, A. Yokoo and T. Tamamura, Appl. Phys. Lett. **78**, 826 (2001).
[19] H. Masuda, H. Asoh, M. Watanabe, K. Nishio, M. Nakao and T. Tamamura, Adv. Mater. **13**, 189 (2001).
[20] J.D. Jannopoulos, R.D. Meade and J.N. Winn, *Photonic Crystals*, Princeton University Press, Princeton, 1995.
[21] H. Masuda, M. Ohya, H. Asoh, M. Nakao, M. Nohtomi and T. Tamamura, Jpn. J. Appl. Phys. **38**, L1403 (1999).
[22] H. Masuda, M. Ohya, K. Nishio, H. Asoh, M. Nakao, M. Nohtomi, A. Yokoo and T. Tamamura, Jpn. J. Appl. Phys. **39**, L1039 (2000).
[23] H. Masuda, M. Ohya, H. Asoh and K. Nishio, Jpn. J. Appl. Phys. **40**, L1217 (2001).
[24] C.R. Martin, Science **266**, 1961 (1994).
[25] J.C. Hulteen and C.R. Martin, J. Mater. Chem. **7**, 1075 (1997).
[26] G. Che, B.B. Lakshmi, E.R. Fisher and C.R. Martin, Nature **393**, 346 (1998).
[27] C.K. Preston and M. Moskovits, J. Phys. Chem. **92**, 2957 (1988).
[28] C.K. Preston and M. Moskovits, J. Phys. Chem. **97**, 8495 (1993).
[29] D. Routkevitch, T. Bigioni, M. Moskovits and J.M. Xu, J. Phys. Chem. **100**, 14037 (1996).
[30] S. Kawai and R. Ueda, J. Electrochem. Soc. **122**, 32 (1975).
[31] C.G. Granqvist, A. Anderson and O. Hunderi, Appl. Phys. Lett. **35**, 268 (1979).
[32] C.A. Huber, T.E. Huber, M. Sadoqi, J.A. Lubin, S. Manalis and C.B. Prater, Science **263**, 800 (1994).
[33] T. Kyotani, L.-F. Tasi and A. Tomita, Chem. Mater. **8**, 2109 (1996).
[34] J. Zhang, L.D. Zhang, X.F. Wang, C.H. Liang, X.S. Peng and Y.W. Wang, J. Chem. Phys. **115**, 5714 (2001).
[35] T. Iwasaki, T. Motoi and T. Den, Appl. Phys. Lett. **75**, 2044 (1999).
[36] J.S. Suh and J.S. Lee, Appl. Phys. Lett. **75**, 2047 (1999).
[37] S.-H. Jeong, H.-Y. Hwang, K.-H. Lee and Y. Jeong, Appl. Phys. Lett. **78**, 2052 (2001).
[38] F. Li, R. Metzger and W.D. Doyle, IEEE Trans. Mag. **33**, 3715 (1997).
[39] S.G. Yang, H. Zhu, G. Ni, D.L. Yu, S.L. Tang and Y.W. Du, J. Phys. D **33**, 2388 (2000).
[40] M. Zheng, L. Menon, H. Zeng, Y. Liu, S. Bandyopadhyyay, R.D. Kirby and D. J. Sellmyer, Phys. Rev. B **62**, 12282 (2000).
[41] K. Nielsch, R.B. Wehrspohn, J. Barthel, J. Kirschner, U. Gosele, S.F. Fischer and H. Kronmuller, Appl. Phys. Lett. **79**, 1360 (2001).
[42] H. Masuda, T. Yanagishita, K. Yasui, K. Nishio, I. Yagi, T. Rao and A. Fujishima, Adv. Mater. **13**, 247 (2001).
[43] T.J. Cheng, J. Jorne and J.-S. Gau, J. Electrochem. Soc. **137**, 93 (1990).
[44] H. Daimon, O. Kitakami, O. Inagoya, A. Sakemoto and K. Mizushima, Jpn. J. Appl. Phys. **29**, 1675 (1990).
[45] H. Masuda H. Tanaka and N. Baba, Chem. Lett. **621** (1990).
[46] H. Masuda, H. Tanaka and N. Baba, Bull. Chem. Soc. Jpn. **66**, 305 (1993).

[47] H. Masuda, K. Nishio and N. Baba, Thin Solid Films **223**, 1 (1993).
[48] H. Masuda, T. Mizuno, N. Baba and T. Ohmori, J. Electroanal. Chem. **368**, 333. (1994).
[49] H. Masuda and K. Fukuda, J. Electroanal. Chem. **473**, 240 (1999).
[50] T. Ohmori, T. Kimura and H. Masuda, J. Electrochem. Soc. **144**, 1286 (1997).
[51] H. Masuda, K. Nishio and N. Baba, Jpn. J. Appl. Phys. **31**, L1775 (1992).
[52] P. Hoyer, N. Baba and H. Masuda, Appl. Phys. Lett. **66**, 2700 (1995).
[53] P. Hoyer and H. Masuda, J. Mater. Sci. Lett. **15**, 1228 (1996).
[54] Y. Lei, C.H. Liang, Y.C. Wu, L.D. Zhang and Y.Q. Mao, J. Vac. Sci. Tech. B **19**, 1109 (2001).
[55] K. Jiang, Y. Wang, J. Dong, L. Gui and Y. Tang, Langmuir **17**, 3635 (2001).
[56] H. Masuda, K. Yasui and K. Nisho, Adv. Mater. **12**, 1031 (2000).
[57] M. Nakao, S. Oku, T. Tamamura, K. Yasui and H. Masuda, Jpn. J. Appl. Phys. **38**, 1052 (1999).
[58] H. Masuda, K. Yasui, Y. Sakamoto, M. Nakao, T. Tamamura and K. Nishio, Jpn. J. Appl. Phys. **40**, L1267 (2001).
[59] Y. Kanamori, K. Hane, H. Sai and H. Yugami, Appl. Phys. Lett. **78**, 142 (2001).
[60] D. Crouse, Y.-H. Lo, A.E. Miller and M. Crouse, Appl. Phys. Lett. **76**, 49 (2000).
[61] J.H. Wu, X.L. Wu, N. Tang, Y.F. Mei, X.M. Bao, Appl. Phys. A **72**, 735 (2001).